

Quenched disorder in the contact process on bipartite sublattices

M. N. Gonzaga,¹ C. E. Fiore,² and M. M. de Oliveira¹

¹*Departamento de Física e Matemática, CAP, Universidade Federal de São João del Rei, Ouro Branco-MG, 36420-000 Brazil*

²*Instituto de Física, Universidade de São Paulo, São Paulo-SP, 05314-970, Brazil*



(Received 18 December 2018; revised manuscript received 8 March 2019; published 29 April 2019)

We study the effects of distinct types of quenched disorder in the contact process with a competitive dynamics on bipartite sublattices. In the model, the particle creation depends on its first and second neighbors and the extinction increases according to the local density. The clean (without disorder) model exhibits three phases: inactive (absorbing), active symmetric, and active asymmetric, where the latter exhibits distinct sublattice densities. These phases are separated by continuous transitions; the phase diagram is reentrant. By performing mean-field analysis and Monte Carlo simulations we show that symmetric disorder destroys the sublattice ordering and therefore the active asymmetric phase is not present. On the other hand, for asymmetric disorder (each sublattice presenting a distinct dilution rate) the phase transition occurs between the absorbing and the active asymmetric phases. The universality class of this transition is governed by the less-disordered sublattice. Finally, our results suggest that random-field disorder destroys the phase transition if it breaks the symmetry between two *active* states.

DOI: [10.1103/PhysRevE.99.042146](https://doi.org/10.1103/PhysRevE.99.042146)

I. INTRODUCTION

In nonequilibrium systems, an absorbing-state phase transition occurs when a control parameter such as a creation or annihilation rate is varied, and the system undergoes a phase transition from a fluctuating state to a frozen state, with no fluctuations (the “absorbing” state). Absorbing-state phase transitions have attracted considerable interest in recent years since they are related to the description of several phenomena such as population dynamics, epidemic spreading, chemical reactions, and others [1–4]. Since the late 2000s, several experimental realizations, e.g., in turbulent liquid crystals [5], driven suspensions [6], superconducting vortices [7], and open quantum systems [8], have highlighted the importance of this kind of phase transition.

In analogy with equilibrium phase transitions [9], it is expected that the critical phase transitions into absorbing states belong to a finite number of universality classes [4]. However, a complete classification of these nonequilibrium classes is still lacking. In general, absorbing-state transitions in models with short-range interactions and in the absence of a conserved quantity or symmetry beyond translational invariance belong to the directed percolation (DP) universality class [10]. On the other hand, models presenting two absorbing states linked by particle-hole symmetry are known fall in the voter model universality class [11]. There are also models that are free of absorbing states but cannot achieve thermal equilibrium because their transition rates violate the detailed balance. An example is the majority vote model [12]. In its ordered phase a Z_2 symmetry is spontaneously broken, leading to Ising-like behavior for spatial dimensions $d \geq 2$.

A few years ago, a spatially structured model that suffers a phase transition to a single absorbing state and also exhibit a broken-symmetry phase was proposed [13]. The model is based in a contact process (CP), where, besides the standard

particle creation and annihilation dynamics, one includes a creation between second neighbors sites and an annihilation proportional to the local density. This results, in addition to the usual absorbing and active (symmetric) phases, in an unusual active asymmetric phase in which the distinct sublattices are unequally populated. A spontaneous symmetry breaking characterizes the reentrant phase transition between the symmetric and asymmetric phases. Mean-field theory (MFT) and simulations revealed the absorbing phase transition belongs to the DP class, whereas the transitions between active phases fall into the Ising universality class, as expected from symmetry considerations. The symmetry-breaking phase transition was proven to be robust for different sublattice interactions [14] and low diffusion particle rates [15].

The inclusion of disorder can affect the critical behavior of nonequilibrium phase transitions dramatically. In real systems, quenched disorder is observed in the form of impurities and defects [16], whereas in a regular lattice it can be included in the forms of random deletion of sites or bonds [17–19] or random spatial variation of the control parameter [20,21]. According to the Harris’s criterion [22], quenched disorder is a relevant perturbation, from the field-theoretical point of view, if $d\nu_{\perp} < 2$, where d is the dimensionality and ν_{\perp} is the correlation length exponent of the pure model. In these cases, quenched uncorrelated randomness induces the emergence of rare regions, typically located $\lambda_c(0) < \lambda < \lambda_c$, the $\lambda_c(0)$ and λ_c being the critical point for the pure and disorder models, respectively. Although globally the whole system is constrained in the subcritical phase, local supercritical regions emerge due to the presence of the disorder. The lifetime of such “active rare regions” grows exponentially with the domain size, usually leading to a slow dynamics, characterized for nonuniversal exponents toward the extinction for some interval of the control parameter below criticality. This behavior characterizes a Griffiths phase (GP) and was verified in DP

models with uncorrelated disorder irrespective to the disorder strength [23,24]. In addition, it was shown this behavior corresponds to the universality class of the random transverse Ising model [23,24]. However, some kinds of correlated disorder do not alter the critical behavior [25–27].

In this work, we provide a step further by investigating the effects of quenched disorder in the phase diagram of the contact processes on sublattices. Following the Harris criterion, disorder should be relevant for the absorbing phase transition, since $\nu_{\perp} = 0.734(4)$ for $d = 2$ in the clean system [23]. On the other hand, for the symmetry-breaking phase transition, the Harris criterion is inconclusive, because it corresponds to a marginal case ($\nu = 1$ for the pure Ising model in $d = 2$) [28]. Here we study distinct kinds of disorder, (i) a random homogeneous and (ii) inhomogeneous deletion of sites, in which the disorder strength is different in each sublattice. Interesting, we show, through mean-field analysis and Monte Carlo simulations, that each one of the above disorder prescriptions yields completely different outcomes.

The remainder of this paper is organized as follows. In the next section we review the model and analyze its mean-field theory. In Sec. III we present and discuss our simulation results; Sec. IV summarizes our conclusions.

II. MODEL AND MEAN-FIELD THEORY

Consider a stochastic interacting particle system, defined on a square lattice of linear size L , where each site can be either occupied by a particle or empty. Each particle creates a new particle in one of its first-neighbor sites with rate λ_1 and in one of its second-neighbor sites with rate λ_2 . Note that in such *bipartite* sublattice, λ_1 is the creation rate in the opposite sublattice, whereas λ_2 is the rate in the same sublattice as the replicating particle. Therefore, *unequal* sublattice occupancies are favored if $\lambda_2 > \lambda_1$. An occupied site is emptied at a rate of unity (independent of its neighboring sites). In addition to the intrinsic annihilation rate of unity, an “inhibition term” proportional to the local density is included in the dynamics. As a consequence of this term, if the occupation fraction ρ_A of sublattice A is much larger than that of sublattice B , for instance, then any particles created in sublattice B will die out quickly, stabilizing the unequal sublattice occupancies.

In order to typify the model properties, we evaluate the macroscopic particle densities of each sublattice A and B given by ρ_A and ρ_B , respectively. In the absorbing (AB) and active symmetric (AS) phases, $\rho_A = \rho_B = 0$ and $\rho_A = \rho_B \neq 0$, respectively. Hence, $\rho = \rho_A + \rho_B$ is a reliable order parameter for absorbing phase transitions. Conversely, for the active asymmetric (AA) phase, it is convenient to calculate the difference of sublattice occupation by $\phi = |\rho_A - \rho_B|$, since ϕ distinguishes from the AS phase, where $\phi = 0$.

The disorder is introduced by means of a fraction Γ of random deletion of sites. We shall consider two cases: the symmetric and asymmetric, in which the sublattice removal is equal ($\Gamma_A = \Gamma_B$) and different ($\Gamma_A \neq \Gamma_B$), respectively. In both cases, the disorder is quenched in space and time, i.e., its position or strength does not change during the evolution of the process. In order to achieve a qualitative portrait of the phase diagram, we begin by employing the one-site MFT. For a lattice with coordination number q , it results in following

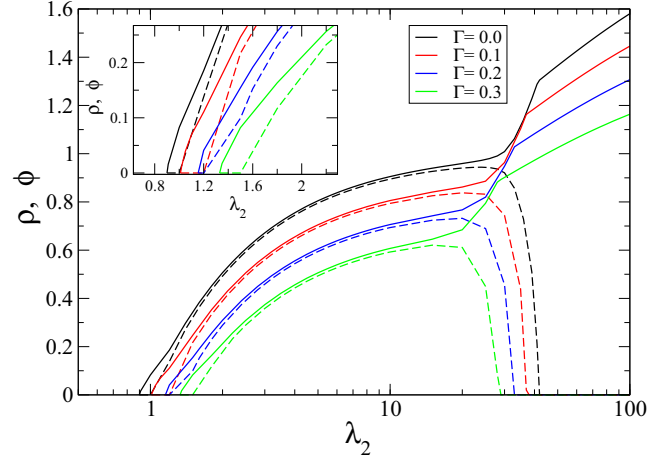


FIG. 1. Mean-field densities ϕ (solid curves) and ρ (dashed) for $\lambda_1 = 0.1$ and $\mu = 2.0$. Inset: Detail of the data close to the absorbing transition (linear scale).

coupled equations:

$$\frac{d\rho_A}{dt} = -[1 + \mu q^2 \rho_B^2] \rho_A + (\lambda_1 \rho_B + \lambda_2 \rho_A)(1 - \Gamma_A - \rho_A) \quad (1)$$

and

$$\frac{d\rho_B}{dt} = -[1 + \mu q^2 \rho_A^2] \rho_B + (\lambda_1 \rho_A + \lambda_2 \rho_B)(1 - \Gamma_B - \rho_B). \quad (2)$$

Let us first consider that the disorder is homogeneously distributed in both sublattices, i.e., $\Gamma_A = \Gamma_B = \Gamma$. In this case, one derives explicit solutions for the densities as

$$\rho = \frac{1}{2k} \left\{ \sqrt{\left(\frac{\lambda_1 + \lambda_2}{2}\right)^2 + 4k[(\lambda_1 + \lambda_2)(1 - \Gamma) - 1]} - \frac{\lambda_1 + \lambda_2}{2} \right\} \quad (3)$$

and

$$\phi = \sqrt{\frac{-[(\lambda_2 - \lambda_1)(1 - \Gamma) - 1 - \lambda_2 \rho - k\rho^2]}{k}}. \quad (4)$$

The mean-field densities ρ and ϕ are plotted as function of λ_2 for distinct values of disorder and fixed $\lambda_1 = 0.1$ in Fig. 1. For all fractions of disorder, the system undergoes a phase transition to the absorbing state at the threshold $\lambda_2 = \lambda_{2,c}^{\text{ABS}}(\Gamma)$, with $\rho = 0$, to the active symmetric phase, where $\rho > 0$ and $\phi = 0$. Note the phase transition moves for larger values of λ_2 when increasing the disorder, as expected. A further increase of λ_2 gives rise to the AS-AA and AA-AS phase transitions at $\lambda_2 = \lambda_{2,c}^{\text{I}}(\Gamma)$ and $\lambda_2 = \lambda_{2,c}^{\text{II}}(\Gamma)$, respectively.

The phase diagram for distinct values of Γ is shown in Fig. 2. The increase of Γ enlarges the absorbing phase and then the AB-AS phase transition moves for larger values of $\lambda_{2,c}^{\text{ABS}}$. In the active phase, the phase diagram is reentrant, and we note the size of the AA phase is reduced when the disorder increases.

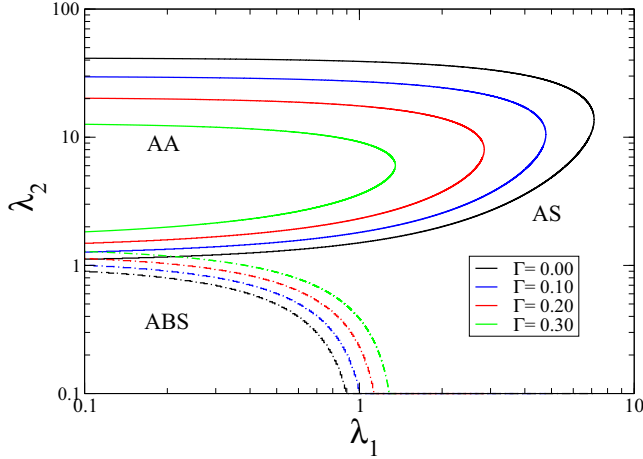


FIG. 2. Phase diagram in the $\lambda_1 - \lambda_2$ plane, for $\mu = 2$, showing absorbing (ABS), active-symmetric (AS), and active-asymmetric (AA), for distinct values of disorder Γ .

The asymmetric disorder case, $\Gamma_A \neq \Gamma_B$, is shown in Fig. 3. MFT indicates the suppression of the AS phase, signed by a smooth change of both of ρ and ϕ at the same $\lambda_{2,c}$. The AS phase is not stable for any value of λ_2 , so that ϕ does not vanish for finite values of λ_2 . So the phase diagram only presents two phases: the absorbing phase and the active asymmetric phase separated by a continuous phase transition.

In the next section, we compare the results from MFT with those evaluated from numerical simulations.

III. RESULTS AND DISCUSSION

A. Methods

We performed extensive Monte Carlo simulations of the model on square lattices with periodic boundaries. The simulation scheme is as follows. First, a site is selected at random. If the site is occupied, it creates a particle at one of its first neighbors with a probability $p_1 = \lambda_1/W$ or at one of its *second* neighbors with a probability $p_2 = \lambda_2/W$. Here

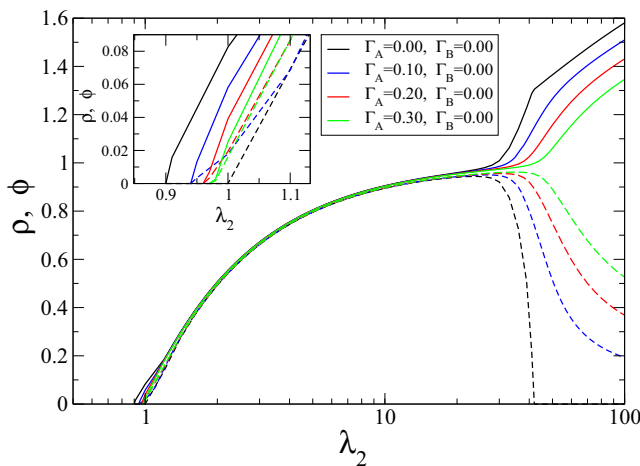


FIG. 3. Mean-field densities ϕ (solid curves) and ρ (dashed) for $\lambda_1 = 0.1$ and $\mu = 2.0$ with asymmetric disorder, $\Gamma_A \neq \Gamma_B$. Inset: Detail of the data close to the absorbing transition (linear scale).

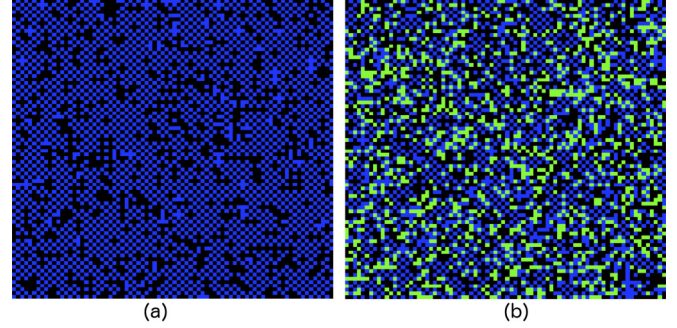


FIG. 4. Typical configurations observed on the bipartite lattice for $\lambda_1 = 0.1$ and $\lambda_2 = 0.1$ for clean $\Gamma = 0.0$ and disordered system $\Gamma = 0.2$. Green, inert sites; blue, occupied sites; black, empty sites. Linear system size $L = 80$ and $\mu = 2.0$.

$W = (1 + \lambda_1 + \lambda_2 + \mu n_1^2)$ is the sum of the rates of all possible events. With a complementary probability $1 - (p_1 + p_2)$, the site is vacated. To improve the efficiency, we choose the sites from a list containing the currently N_{occ} occupied sites; accordingly, the time is incremented by $\Delta t = 1/N_{\text{occ}}$ after each event. For simulations in the subcritical and critical absorbing regime, we sample the quasistationary (QS) regime using the simulation method detailed in Ref. [29]. In order to draw a comparison with the results from MFT, in all cases we take $\mu = 2.0$.

B. Symmetric disorder

We begin by analyzing the symmetric case, where $\Gamma_A = \Gamma_B = \Gamma$. In Fig. 4, we show typical configurations observed on the bipartite lattice for $\lambda_1 = 0.1$ and $\lambda_2 = 0.1$, for clean $\Gamma = 0$ and disordered system $\Gamma = 0.2$.

Figure 5 shows the densities of ρ and ϕ on a square lattice with linear system size $L = 80$. As expected, the absorbing phase transition occurs at a higher value of λ_2 when disorder is introduced. We also observe that increasing the fraction of disorder reduces the possibility of an AA phase, since the values of ϕ reduces when we increase the fraction of disorder.

In order to clarify the effects of disorder on the stability of the AA phase, we analyze the dependence of the order

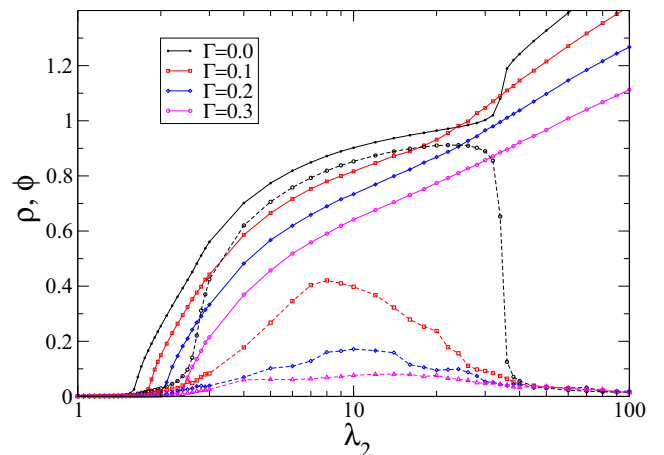


FIG. 5. Order parameters ρ and ϕ for distinct (symmetric) Γ 's vs. λ_2 for $\mu = 2$ and $\lambda_1 = 0.1$. Linear system size $L = 80$.

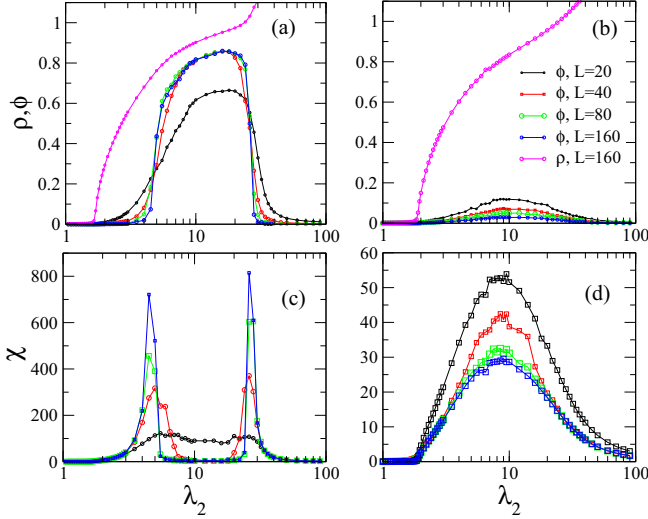


FIG. 6. Quasistationary densities ϕ and ρ vs. λ_2 , for $\mu = 2$ and $\lambda_1 = 0.1$, for the clean system (a) and for $\Gamma = 0.1$ (b). Scaled variance χ of the order parameter ϕ vs. λ_2 for $\mu = 2$ and $\lambda_1 = 0.1$, for the clean system (c), and for $\Gamma = 0.1$ (d).

parameter ϕ with the linear system size L . In Fig. 6, we compare the clean model with the disordered system, with $\Gamma = 0.1$. Figures 6(a) and 6(b) show the order parameter ρ and ϕ versus λ_2 for distinct systems sizes. While for the clean version the AA phase and the reentrant phase transition are observed for all system sizes [see Fig. 6(a)], the disordered system shows a remarkably different picture, in which the sublattice occupations become equivalent for large L . Therefore, we conclude that ϕ vanishes when $L \rightarrow \infty$ and the AA phase is suppressed by the disorder. Such behavior is reinforced by analyzing the order parameter variance $\chi = L^2(\langle \phi^2 \rangle - \langle \phi \rangle^2)$, as shown in Figs. 6(c) (clean) and 6(d) (disordered). In contrast to the clean system, in which χ diverges nearby the transitions AB-AA and AA-AB as $L \rightarrow \infty$, no divergence is verified in such case. So, in contrast to the MFT predictions, we observe that symmetric disorder forbids the stability of AA phase and therefore the disordered system does not show symmetry breaking.

One important point to mention is that the random dilution *locally* breaks the symmetry between the sublattices even in this case, where $\Gamma_A = \Gamma_B$. Therefore, the dilution acts as a “random-field” disorder for the symmetry breaking between the sublattices. Recently, it was shown that nonequilibrium phase transitions persists in the presence with random-field disorder that locally breaks the symmetry between two absorbing states [30–32]. In this contrast, our results reveal that random-field disorder destroys the phase transition if it breaks the symmetry between two *active* states. This behavior is analogous to that observed in low-dimensional *equilibrium* systems, where random-field disorder is known to prevent spontaneous symmetry breaking [33,34].

Now let us characterize the absorbing phase transition in the disordered system. For locating the critical creation rate $\lambda_{2,c}$, we study the time evolution of the number of active particles $n(t)$ starting from an initial configuration the simulation with one pair of neighboring active particles. The critical value $\lambda_{2,c}$ can be estimated as the threshold λ_2

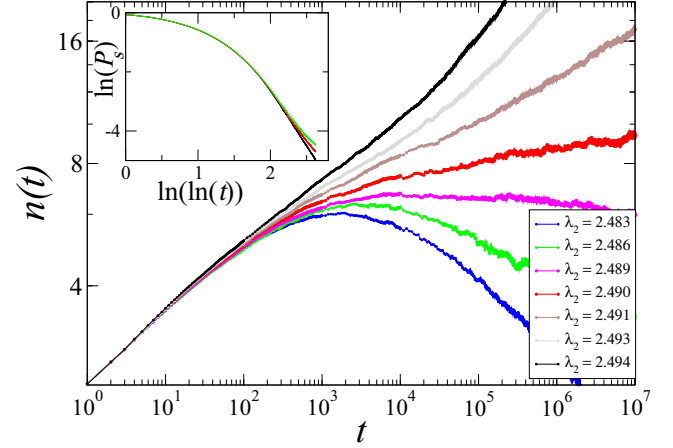


FIG. 7. Number of active particles n for $\Gamma = 0.3$, $\mu = 2$, and $\lambda_1 = 0.1$. Inset: Survival probability for $\lambda_2 = 2.489$, 2.490, and 2.491.

separating asymptotic growth from the decay toward the absorbing phase.

Figure 7 exemplifies the results for $\Gamma = 0.3$ in which $\lambda_{2,c} = 2.490(1)$. We observe that, analogously to the diluted CP, the critical behavior presents activated dynamic scaling, with

$$n(t) \sim \ln(t/t_0)^\theta \quad (5)$$

and the survival probability

$$P_s \sim \ln(t/t_0)^{-\delta}. \quad (6)$$

From the data in Fig. 7, we estimate $\ln(t_0) = 3.0(5)$, and $\theta = 0.21(4)$, in agreement with the value $\theta = 0.15(3)$, obtained in Ref. [24]. From the data shown in the inset of Fig. 7, we find $\delta = 2.1(3)$, very close to the value $\delta = 1.9(2)$ observed for the usual CP with random dilution, indicating that the critical behavior of the disordered model belongs to the universality class of the diluted CP [24,35].

Combining the activated scaling relations for $n(t)$ and $P_s(t)$, Eqs. (5) and (6), we find that

$$n \sim P_s^{-\delta/\theta} \quad (7)$$

at criticality. This relation does not depend on t_0 and is useful to check our estimate of the critical point. In Fig. 8, we plot n as function of P_s and observe a power law that at $\lambda_2 = 2.490$, while the curves for $\lambda_2 = 2.491$ ($\lambda_2 = 2.489$) veers up (down), thus confirming the accuracy of our estimate for the critical point. At criticality, we found the exponent ratio $\delta/\theta = 0.09(2)$, in coherence with the values of δ and θ obtained from the data in Fig. 7. This value is also in agreement with the value $\delta/\theta = 0.075(5)$ obtained for the diluted contact process in Ref. [35].

In the active-dynamical scenario, the lifetime of the process follows,

$$\ln \tau \sim L^\psi, \quad (8)$$

where ψ is a universal exponent. From the data in the inset of Fig. 8, we found $\psi = 0.44(5)$, close to the value $\psi = 0.51(6)$ obtained for the diluted CP [24].

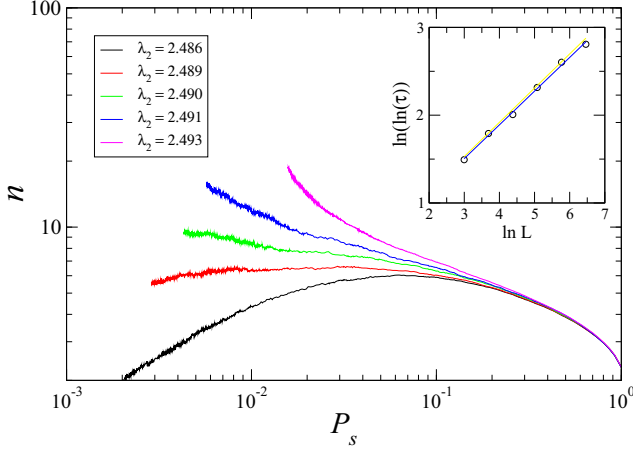


FIG. 8. Log-log plot of the number of occupied sites n as a function of the survival probability P_s obtained from spreading simulations. Inset: Finite-size scaling of the lifetime of the QS state τ for $\Gamma = 0.3$, $\mu = 2$, and $\lambda_1 = 0.1$.

Finally, another important effect that disorder can induce in absorbing phase transitions is the emergence of Griffiths phases [36]. A Griffiths phase is a region inside the subcritical phase where the long-time decay of ρ toward the extinction is algebraic (with nonuniversal exponents) rather than exponential. In Fig. 9, we present results from initial decay simulations, where the system starts its dynamics from a fully occupied lattice. We observe the existence of a range of values of λ_2 in the subcritical regime where the long-time behavior of the density decays as a power law,

$$\rho(t) \sim t^{-2/z'}, \quad (9)$$

with the nonuniversal dynamical exponents z' following

$$z' \sim |\lambda_2 - \lambda_{2,c}|^{-\psi v_\perp}, \quad (10)$$

where $\lambda_{2,c}$ is the critical value of the control parameter λ_2 [24]. In the inset of Fig. 9 we observe that z' diverges when λ_2

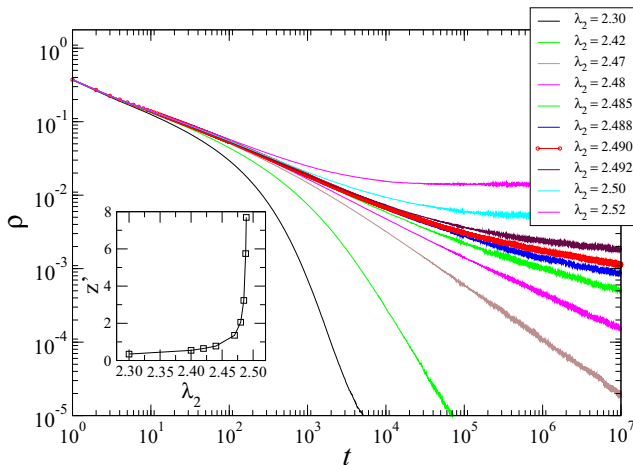


FIG. 9. Initial decay simulations: Particle density ρ vs. t for $\mu = 2$ and $\lambda_1 = 0.1$ for symmetric disorder case, with $\Gamma = 0.3$ (linear system size $L = 2000$). Inset: Dynamical exponent z' as a function of λ_2 .

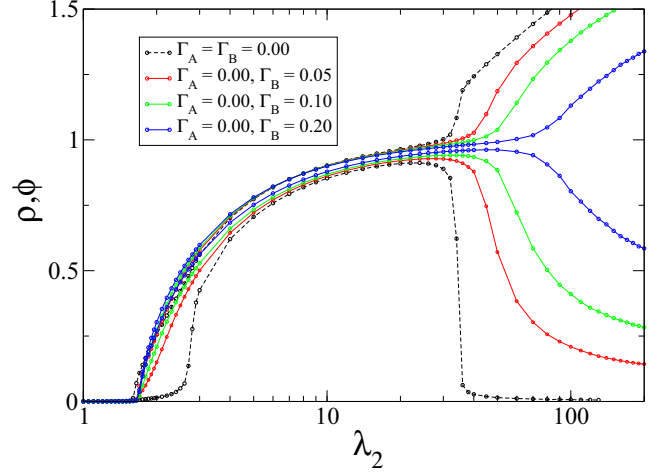


FIG. 10. For $L = 80$ and asymmetric disorder: Order parameters ϕ and ρ for $\mu = 2$ and $\lambda_1 = 0.1$ for distinct Γ_A and Γ_B .

approaches $\lambda_{2,c} = 2.490$. From these data, we obtain $\psi v_\perp = 0.60(1)$, in good agreement with the value $\psi v_\perp \approx 0.61$ reported in Ref. [24] for the diluted CP.

To summarize, our results for the effects of symmetric disorder are in agreement with the predictions from the Harris criterium, since $v_\perp = 0.734(4)$ for $d = 2$ in the clean system, and therefore the disorder is relevant for the absorbing phase transition [23]. Similar trends have been observed for lower values of Γ , although larger crossover times toward the infinite-random behavior are expected in such cases [23,24].

C. Asymmetric disorder

Now we investigate the effects of asymmetric disorder in which disorder strengths is different in each sublattice. Here the asymmetric disorder explicitly breaks the symmetry between the two sublattices. Therefore, the active state always exhibit different densities in both sublattices. This is exemplified in Fig. 10 for $\Gamma_1 = 0$ and distinct values of Γ_2 . We note that even a very small asymmetric disorder ($\Gamma_2 = 0.05$), the AS phase is suppressed and only less disordered sublattice is populated. Therefore, only a phase transition between the inactive and the asymmetric phase is presented, whose critical behavior is ruled by the less disordered sublattice. In all these cases, we observe that at criticality, $\rho \sim L^{-\beta/v_\perp}$ and the lifetime $\tau \sim L^{-z}$. For example, for $\Gamma_2 = 0.2$, shown in Fig. 11, we find $\beta/v_\perp = 0.81(2)$ and $z = 1.75(3)$, in agreement with the DP values $\beta/v_\perp = 0.797(3)$ and $z = 1.7674(6)$. The inset shows the moment ratios of the order parameter, $m = \langle \rho \rangle^2 / \langle \rho^2 \rangle$ goes to a universal value $m = 1.33(1)$ at criticality, in comparison to the known DP value $m = 1.3264(5)$ [13].

D. Phase diagrams

Our simulation results for the effects of disorder are resumed in the phase diagrams shown in Fig. 12. In Fig. 12(a), the clean system exhibits, besides the absorbing phase, a reentrant active asymmetric phase (with $\phi > 0$) inside the active symmetric phase. In Ref. [13], it was shown that the active-absorbing phase belongs to the DP universality class, while the AA-AS symmetry-breaking phase transition is Ising-like.

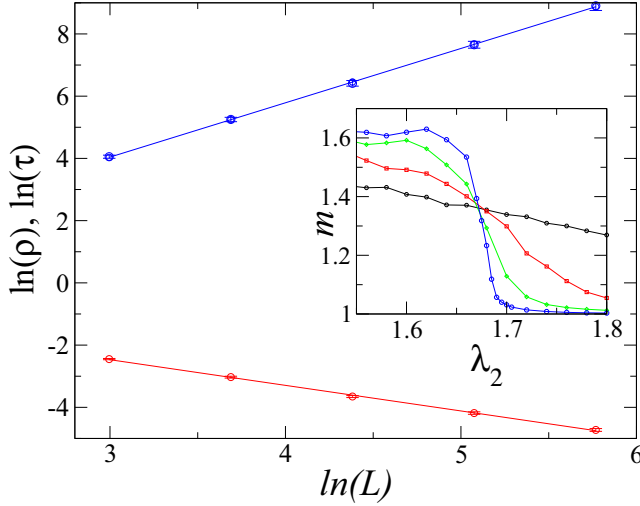


FIG. 11. Asymmetric disorder, with $\Gamma_1 = 0.0$ and $\Gamma_2 = 0.2$: Scaled critical QS density of active sites $\ln \rho$ (bottom) and scaled lifetime of the QS state $\ln \tau$ (top) versus $\ln L$. Inset: Moment ratio m versus λ_2 on a square lattice. Parameters: $\mu = 2$ and $\lambda_1 = 0.1$

The effects of asymmetric disorder in the phase diagram are shown in Figs. 12(b) and 12(c). We note that the AS phase vanishes, and there are only two phases, the absorbing and the AA phases. The universality class of the transition between these phases is governed by the less-disordered sublattice. So, while in Fig. 12(b), the phase transition belongs to the DP universality class, in Fig. 12(c) it belongs to the universality class of the diluted CP.

Finally, if the disorder is symmetric, as Fig. 12(d), we note that the AA phase vanishes, and the absorbing-AS phase transition belongs to the class of the diluted CP. This system exhibits activated scaling and Griffiths phases as shown in detail in Sec. III B.

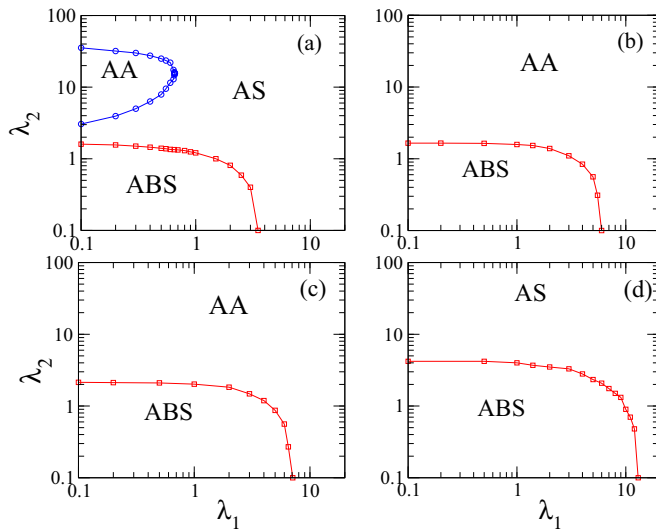


FIG. 12. Phase diagrams for (a) clean system, (b) $\Gamma_A = 0$ and $\Gamma_B = 0.3$, (c) $\Gamma_A = 0.1$ and $\Gamma_B = 0.3$, and (d) $\Gamma_A = \Gamma_B = 0.3$ ($\mu = 2$ in all cases).

IV. CONCLUSIONS

In this work, we have investigated the effects of quenched disorder in the phase diagram of the competitive contact processes on sublattices. Through mean-field analysis and Monte Carlo simulations, we have studied distinct types of disorder, (i) a random *homogeneous* deletion of sites (ii) an asymmetrical disorder, in which the disorder strength is different in each sublattice. Interestingly, each one of the above disorder prescriptions yields different outcomes.

We observe that in case (i), the disorder destroys the asymmetric active phase and therefore the symmetry-breaking phase transition. So there are only two phases, the absorbing and the active (symmetric) phases. The absorbing-active phase transition exhibited belongs to the universality class of the disordered contact process. Effects related to an infinite randomness fixed point are observed, such as activated dynamics and Griffiths phases in the subcritical regime.

A distinct behavior is observed if each sublattice has a different disorder strength. In such a case, the symmetrical active phase is not stable, and we observe a phase transition directly from the active asymmetric phase to the absorbing phase. The critical behavior in this case is governed by the sublattice with less disorder; for instance, if one of the sublattices has no disorder, then the phase transition will fall in the DP class.

One important point to mention is that, in both cases above, there is no symmetry-breaking phase transition. The dilution works as a “random-field” disorder for the symmetry breaking between the sublattices, since it *locally* breaks the symmetry between the sublattices even when the disorder is globally symmetric (i.e., when $\Gamma_A = \Gamma_B$). When the disorder is asymmetric, it explicitly breaks the symmetry between the two sublattices. Therefore in the present work the random-field disorder suppresses the phase transition between the active phases, since it breaks the symmetry between them. This is in contrast to the behavior observed in the presence of random-field disorder that locally breaks the symmetry between two *absorbing* states [30–32], where nonequilibrium phase transitions persist.

A natural extension of the present work would be the study of the effects of temporal disorder [37–40] on the robustness of the symmetry-breaking phase transition and in its critical behavior. It is important to mention that, besides the theoretical interest in the field of nonequilibrium phase transitions, suppression of activity at the nearest neighbors of active sites resembles biological lateral inhibition, known to be important in the visual system of many animals [41]. Also, our work can be useful to understand the effects of heterogeneities in extended systems showing *checkerboard* pattern distributions such as mutually exclusive species co-occurrences [42].

ACKNOWLEDGMENTS

This work was supported by CNPq and FAPEMIG, Brazil. C.E.F. acknowledges financial support from Fapesp under grant Projeto Fapesp 2018/02405-1.

- [1] J. Marro and R. Dickman, *Nonequilibrium Phase Transitions in Lattice Models* (Cambridge University Press, Cambridge, 1999).
- [2] H. Hinrichsen, *Adv. Phys.* **49**, 815 (2000).
- [3] M. Henkel, H. Hinrichsen, and S. Lubeck, *Non-Equilibrium Phase Transitions Volume I: Absorbing Phase Transitions* (Springer-Verlag, The Netherlands, 2008).
- [4] G. Ódor, *Rev. Mod. Phys.* **76**, 663 (2004).
- [5] K. A. Takeuchi, M. Kuroda, H. Chaté, and M. Sano, *Phys. Rev. Lett.* **99**, 234503 (2007).
- [6] L. Corté, P. M. Chaikin, J. P. Gollub, and D. J. Pine, *Nat. Phys.* **4**, 420 (2008).
- [7] S. Okuma, Y. Tsugawa, and A. Motohashi, *Phys. Rev. B* **83**, 012503 (2011).
- [8] R. Gutiérrez, C. Simonelli, M. Archimi, F. Castellucci, E. Arimondo, D. Ciampini, M. Marcuzzi, I. Lesanovsky, and O. Morsch, *Phys. Rev. A* **96**, 041602 (2017).
- [9] N. Goldenfeld, *Lectures on Phase Transitions and the Renormalization Group* (Addison-Wesley, New York, 1992).
- [10] H. K. Janssen, *Z. Phys. B* **42**, 151 (1981); P. Grassberger, *ibid.* **47**, 365 (1982).
- [11] I. Dornic, H. Chaté, J. Chave, and H. Hinrichsen, *Phys. Rev. Lett.* **87**, 045701 (2001).
- [12] M. J. de Oliveira, *J. Stat. Phys.* **66**, 273 (1992).
- [13] M. M. de Oliveira and R. Dickman, *Phys. Rev. E* **84**, 011125 (2011).
- [14] S. Pianegonda and C. E. Fiore, *J. Stat. Mech.* (2014) P05008.
- [15] M. M. de Oliveira and C. E. Fiore, *J. Stat. Mech.* (2017) 053211.
- [16] H. Hinrichsen, *Braz. J. Phys.* **30**, 69 (2000).
- [17] A. J. Noest, *Phys. Rev. Lett.* **57**, 90 (1986).
- [18] A. G. Moreira and R. Dickman, *Phys. Rev. E* **54**, R3090 (1996); R. Dickman and A. G. Moreira, *ibid.* **57**, 1263 (1998).
- [19] T. Vojta and M. Y. Lee, *Phys. Rev. Lett.* **96**, 035701 (2006).
- [20] M. Bramson, R. Durrett, and R. Schonmann, *Ann. Prob.* **19**, 960 (1991).
- [21] M. S. Faria, D. J. Ribeiro, and S. R. Salinas, *J. Stat. Mech.* (2008) P01022.
- [22] A. B. Harris, *J. Phys. C* **7**, 1671 (1974).
- [23] M. M. de Oliveira and S. C. Ferreira, *J. Stat. Mech.: Theor. Exp.* (2008) P11001.
- [24] T. Vojta, A. Farquhar, and J. Mast, *Phys. Rev. E* **79**, 011111 (2009).
- [25] M. M. de Oliveira, S. G. Alves, S. C. Ferreira, and R. Dickman, *Phys. Rev. E* **78**, 031133 (2008).
- [26] H. Barghathi and T. Vojta, *Phys. Rev. Lett.* **113**, 120602 (2014).
- [27] M. M. de Oliveira, S. G. Alves, and S. C. Ferreira, *Phys. Rev. E* **93**, 012110 (2016).
- [28] P. H. L. Martins and J. A. Plascak, *Phys. Rev. E* **76**, 012102 (2007).
- [29] M. M. de Oliveira and R. Dickman, *Phys. Rev. E* **71**, 016129 (2005); *Braz. J. Phys.* **36**, 685 (2006).
- [30] H. Barghathi and T. Vojta, *Phys. Rev. Lett.* **109**, 170603 (2012).
- [31] C. Borile, A. Maritan, and M. A. Muñoz, *J. Stat. Mech.: Theory Exp.* (2013) P04032.
- [32] H. Barghathi and T. Vojta, *Phys. Rev. E* **93**, 022120 (2016).
- [33] Y. Imry and S.-K. Ma, *Phys. Rev. Lett.* **35**, 1399 (1975).
- [34] M. Aizenman and J. Wehr, *Phys. Rev. Lett.* **62**, 2503 (1989).
- [35] A. H. O. Wada and M. J. de Oliveira, *J. Stat. Mech.* (2017) 043209.
- [36] J. Hooyberghs, F. Iglói, and C. Vanderzande, *Phys. Rev. E* **69**, 066140 (2004).
- [37] F. Vazquez, J. A. Bonachela, C. López, and M. A. Muñoz, *Phys. Rev. Lett.* **106**, 235702 (2011).
- [38] R. Martínez-García, F. Vazquez, C. López, and M. A. Muñoz, *Phys. Rev. E* **85**, 051125 (2012).
- [39] M. M. de Oliveira and C. E. Fiore, *Phys. Rev. E* **94**, 052138 (2016).
- [40] C. E. Fiore, M. M. de Oliveira, and J. A. Hoyos, *Phys. Rev. E* **98**, 032129 (2018).
- [41] W. Lytton, *From Computer to Brain* (Springer-Verlag, New York, 2002).
- [42] E. F. Connor, M. D. Collins, and D. Simberloff, *Ecology* **94**, 2403 (2013).